

# Structure of unstable light nuclei

D.J. Millener<sup>1</sup>

*Physics Department, Brookhaven National Laboratory, Upton, NY 11973, USA*

---

## Abstract

The structure of light nuclei out to the drip lines and beyond up to  $Z \sim 8$  is interpreted in terms of the shell model. Special emphasis is given to the underlying supermultiplet symmetry of the p-shell nuclei which form cores for neutrons and protons added in sd-shell orbits. Detailed results are given on the wave functions, widths, and Coulomb energy shifts for a wide range of non-normal parity states in the p-shell.

*Key words:* Shell-model; supermultiplet symmetry; weak-coupling model; Nilsson model; level widths; Coulomb energies

*PACS:* 21.60.Cs; 27.20.+n

---

## 1 Introduction

The light nuclei have long provided a testing ground for nuclear models. Most of the basic ideas were already in place by the end of the 1950's as can be seen from a perusal of the proceedings of the Kingston conference in 1960 [1] and a recent history of the development of our understanding of nuclear structure by Wilkinson [2] (this reference lists the important papers and outlines subsequent developments).

As far as the shell model was concerned [3], the fractional parentage coefficients for the p shell in both  $jj$  and LS coupling had been available since the early 50's but the slow development of electronic computing meant that it was the mid 50's before the first diagonalizations (up to  $22 \times 22$ ) for  $(sd)^3$  by Elliott and Flowers [4] and for the complete p shell by Kurath [5] were published. Excitations across major shells with proper elimination of spurious centre-of-mass states were considered by Elliott and Flowers for  $A = 16$  [6]. This paper

---

<sup>1</sup> E-mail: millener@bnl.gov

also provided a microscopic description of giant dipole strength in  $^{16}\text{O}$ . The presence of non-normal-parity states at low excitation energy was known in  $^{19}\text{F}$  at 110 keV (suggested as the weak coupling of a  $0p_{1/2}$  proton hole to  $^{20}\text{Ne}$  [7]), in  $^{13}\text{N}$  at 2.4 MeV (the weak coupling of an  $1s_{1/2}$  proton to  $^{12}\text{C}$  [8]), and a  $\frac{1}{2}^+$  ground state for  $^{11}\text{Be}$  was strongly suspected [9,10]. In the appropriate limits, the close connection between the shell model and the cluster model and between the shell model and the collective (Nilsson) model was known, the latter being made clear from Elliott's formulation of the  $\text{SU}(3)$  shell model [11]; also the need for and basic origin of effective interactions and charges.

Of course, the information on spins, parities, and other properties of nuclear levels was still rather sparse [12]. The next few decades brought a rapid filling out of this basic knowledge, as may be traced through the succeeding tabulations [13]. In recent years, the advent of radioactive beam facilities has greatly improved our knowledge of the structure of nuclei far from stability, out to the drip lines and beyond in the case of light nuclei.

The purpose of this paper is to interpret the structure of light nuclei up to  $Z \sim 8$  in terms of the shell model, using where necessary its relation to the cluster, Nilsson, and weak-coupling models to provide a simple understanding of the structure. In principle the shell model is complete and in practice it can be used phenomenologically to correlate rather precisely the systematics of nuclear properties over considerable ranges of mass number. For some mass numbers, the tabulations are up to 12 years out of date but the general flavour of advances in the field can be obtained from recent major conferences such as ENAM98 [14], recent reviews on specific topics [15–18], and the most recent references to specific nuclei (given later).

## 2 Structure Calculations

Large scale  $0\hbar\omega$  shell-model calculations have now reached close to the middle of the  $pf$  shell [19]. These results, obtained using a  $G$ -matrix interaction with monopole modifications, have also been used to benchmark shell-model Monte Carlo calculations [20,21] which can be used for even larger model spaces. Both types of calculations have been employed for neutron rich nuclei involving both the  $sd$  and  $pf$  shells [20,22] where some ground states involve the excitation of pairs of neutrons across the  $N = 20$  shell closure. Similar violations of the normal shell ordering occur at  $N = 8$  [23]. As is discussed later, the structure of such nuclei can be described by shell-model calculations which use two-body matrix elements fitted to  $0\hbar\omega$ ,  $1\hbar\omega$ , and  $2\hbar\omega$  configurations in the  $A = 10 - 22$  nuclei [24].

Binding energy effects are not taken account in the shell-model calculations

themselves. Rather, Woods-Saxon radial wave functions evaluated at the physical separation energy are used to calculate transition matrix elements. Further improvement is possible by using the shell-model structure information to set up radial equations for the appropriate one-nucleon overlap functions [25].

Microscopic cluster models generally include the correct degrees of freedom to describe extended, loosely bound systems without violating the Pauli principle or introducing spurious center of mass excitations. Recent developments include solutions by the stochastic variational method [26], antisymmetrized molecular dynamics [27], molecular orbital methods [28], and generator coordinate methods [29]. Such calculations use saturating central forces, such as the Volkov or Minnesota interactions, augmented by a spin-orbit interaction. Parameters, such as the space-exchange mixture, are often varied on a case-by-case basis to reproduce energies with respect to thresholds for states of interest.

Finally, there have been great advances in the theoretical treatment of few-nucleon systems [30] and some of the techniques can be used for p-shell nuclei. In particular, variational Monte Carlo and Green's function Monte Carlo results using realistic free NN interactions and phenomenological but theoretically motivated NNN interactions have been published up to  $A = 8$  [31]. Very impressive agreement with experiment has been obtained for  ${}^6\text{Li}(e, e'){}^6\text{Li}$  form factors [32] and for  ${}^7\text{Li}(e, e'){}^6\text{He}$  momentum distributions and spectroscopic factors [33]. The last result emphasises the essential quasi-particle nature of the shell model and the role played by (short-range) correlations [34,35].

### 3 The p-shell nuclei

A comprehensive description and understanding of the structure of p-shell ( $0\hbar\omega$ ) states is important both in its own right and because neutrons in sd-shell orbits are added to p-shell cores as one moves towards the drip line or higher in excitation energy for many light elements. In fact, there is often near degeneracy, or coexistence, of nominally  $0\hbar\omega$ ,  $1\hbar\omega$ ,  $2\hbar\omega$ , etc. states.

It should be noted that Barrett and collaborators have performed *ab initio* no-core shell-model calculations in at least  $4\hbar\omega$  spaces up to  $A = 12$  with effective interactions derived microscopically from realistic NN interactions [36]. The spectra for known p-shell levels are good. To date, however, the non-normal-parity states, and consequently all multi- $\hbar\omega$  states, are predicted too high in energy.

At the beginning of the p-shell, the wave functions for the observed states have long been known to be close to the supermultiplet (LS) limit in which

the orbital wave functions are classified by the  $SU(3) \supset O(3)$  quantum numbers  $(\lambda \mu) K_L L$  ( $\lambda = f_1 - f_2$  and  $\mu = f_2 - f_3$  from the spatial symmetry  $[f] = [f_1 f_2 f_3]$ ) and the  $SU(4) \supset SU(2) \times SU(2)$  quantum numbers  $[\tilde{f}] \beta T S$  (see, e.g., Barker's wave functions for  $A = 6 - 9$  [37]). In fact, the supermultiplet scheme provides an excellent basis for an understanding of the structure and energetics of all p-shell nuclei. This can be demonstrated from an analysis of a p-shell Hamiltonian obtained by fitting 34 levels for  $A = 10 - 12$ . In the fit only a limited number of well-determined linear combinations of the parameters were allowed to vary. The single-particle energies were always well determined, as were the central matrix elements with the exception of the singlet-odd interaction. The strength of the tensor interaction was fixed to obtain, in competition with the spin-orbit interaction, the sign and magnitude of the  ${}^3S_1$  and  ${}^3D_1$  mixing in the  ${}^6\text{Li}$  and  ${}^{14}\text{N}$  ground states necessary to explain the small Gamow-Teller matrix element in  ${}^{14}\text{C}$   $\beta$  decay and a small negative quadrupole moment for  ${}^6\text{Li}$ . The spin-orbit splitting of 4.78 MeV (3.49 MeV for a similar  $A = 6 - 9$  fit) is much larger than that of the Cohen-Kurath interactions [38] for the light p-shell nuclei.

The calculations were performed with an  $SU(3)$  shell-model code based on the formalism of French [39] adapted for  $SU(3)$  [40]. From the coefficients of the six (00) and (22)  $SU(3)$  tensors which define the central interaction, it is possible to find the coefficients of the 5  $SU(4)$  invariants which characterize the symmetry-preserving part of the interaction [41]. This decomposition, including the contribution from the one-body centroid, is given below. The coefficient of the sixth tensor is essentially zero so that the central interaction is almost perfectly symmetry preserving.

$$H = 1.563n - 1.709I_{ij} - 3.908P_{ij} + 0.590L^2 - 1.078S^2 + 0.594T^2 \quad (1)$$

For the spatial symmetry  $[f] = [f_1 f_2 f_3]$ , the expectation value of the space-exchange interaction  $P_{ij}$  is  $\frac{1}{2} \sum_i f_i (f_i - 2i + 1) = n_s - n_a$ , where  $n_s - n_a$  is the difference between the number of symmetric and antisymmetric pairs.

The binding energies given by Eq. (1) for the lowest p-shell states in nuclei of interest are shown in Fig. 1. As can be seen, the dominant contributor to the spacing between the nuclei with different isospins is the space-exchange interaction. These spacings are more or less conserved when the non-central interactions are switched on with admixings of  $< 30\%$  (often much less) of lower symmetry into the lowest states throughout the p shell. For example, the ground state of  ${}^{12}\text{C}$  is typically  $\sim 80\%$  [44] symmetry (LS = 00), as we might expect for a nucleus that we can think of as 3  $\alpha$  particles, with a [431] admixture (LS = 11) of  $\sim 16\%$  induced by the spin-orbit interaction. This admixture provides the Gamow-Teller (GT) transition strengths in the  $\beta$  decay of  ${}^{12}\text{B}$  or  ${}^{12}\text{N}$ . The closed  $p_{3/2}$  shell forms  $< 40\%$  of the ground-state

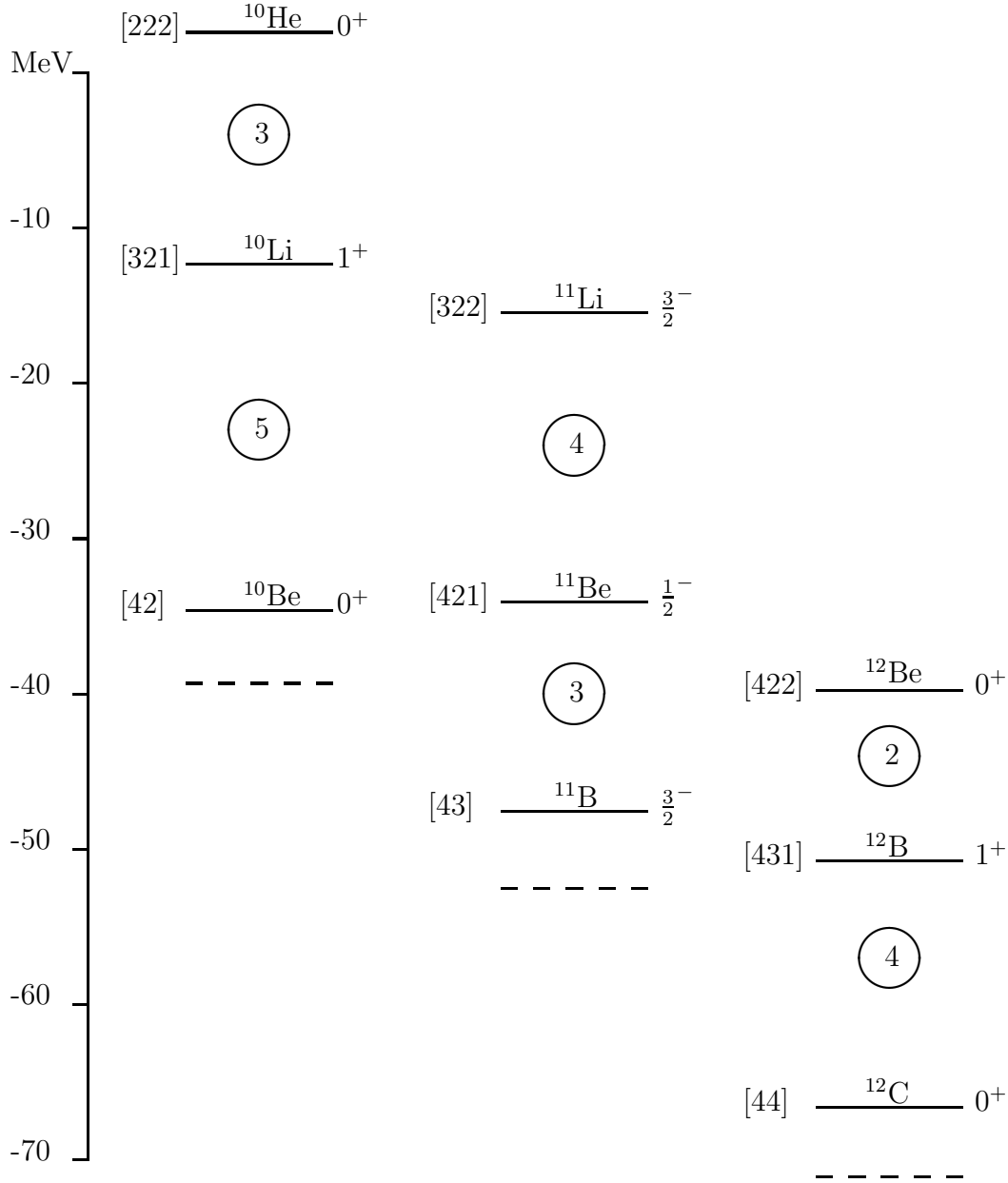


Fig. 1. The solid lines labelled by spatial symmetry, nucleus, and the spin-parity of the lowest p-shell state give the Coulomb-corrected binding energies with respect to  $^4\text{He}$  for the central part of a p-shell interaction fitted to 34 level energies from the  $A = 10 - 12$  nuclei. The dotted lines represent the corresponding experimental binding energies for the lowest state of each mass number. These energies are well reproduced when the non central interactions are included, with the dominant effect (typically an energy gain of  $\sim 4$  MeV) coming from the one-body spin-orbit interaction. The circled numbers give differences in the eigenvalues of the space-exchange operator for the spatial symmetries  $[f]$  shown.

wave function (the overlap of  $p_{3/2}^8$  with [44] is only  $\sqrt{5/81}$  [8]).

With regard to the smaller angular momentum and isospin dependent terms in Eq. (1), the  $L^2$  term gives the well-known  $L(L+1)$  dependence exhibited by the p-shell interaction. The influence of the  $S^2$  and  $T^2$  terms can be seen in the strong low-energy Gamow-Teller transitions observed in the high  $Q_\beta$  decays of  ${}^8\text{He}$ ,  ${}^9\text{Li}$ , and  ${}^{11}\text{Li}$ . In the case of  ${}^8\text{He}$  decay ( $Q_\beta = 10.653$  MeV) [42], the lowest three  $1^+$  states of  ${}^8\text{Li}$  have small GT matrix elements because the wave functions have dominantly [31] spatial symmetry (mixed LS = 10, 11, 21) but the  $1_4^+$  state near 9 MeV has a large GT matrix element corresponding to the transition  $|[22] L=0 S=0 T=2\rangle \rightarrow |[22] L=0 S=1 T=1\rangle$ . The intensities of these configurations in the initial and final states are 74.0% and 71.5%, respectively, and the influence of the  $S^2$  and  $T^2$  terms in lowering the  $1_4^+$  state below the analog of the initial state at 10.822 MeV in  ${}^8\text{Li}$  is clear. Similarly, in the decay of  ${}^{11}\text{Li}$  ( $Q_\beta = 20.7$  MeV) [43,44], the strong transition is between states of [322] symmetry with  $L = 1$  to a state just above 18 MeV in  ${}^{11}\text{Be}$ . The main candidate is a  $\frac{5}{2}^-$  state predicted at 17.8 MeV with 87% by intensity of [322] symmetry with  $S = \frac{3}{2}$ . An essentially degenerate  $\frac{3}{2}^-$  level is also predicted to carry significant GT strength. The predicted p-shell GT values are strongly quenched by large  $(sd)^2$  admixtures in the  ${}^{11}\text{Li}$  ground state [45,46].

Another important aspect of the underlying supermultiplet symmetry for p-shell states is how it influences parentage, single-nucleon or multi-nucleon, and therefore the magnitudes of cross sections for transfer reactions and the widths of unbound levels. Before turning to p-shell properties of interest for some of the He, Li, and Be isotopes, a brief discussion of these matters is given in the following subsection.

### 3.1 Parentages and widths

For unbound states with modest widths an excellent way to estimate the nucleon decay width at energy  $E_N$  above threshold is given by

$$\Gamma_N = C^2 S \Gamma^{sp}(E_N) , \quad (2)$$

where  $E_N - i\frac{1}{2}\Gamma^{sp}$  is the complex resonance energy for a potential well [47], e.g. a Woods-Saxon well with  $r_0 \sim 1.25$  fm and  $a \sim 0.6$  fm, with a depth chosen to reproduce  $E_N$ . The spectroscopic factor  $S$  is the square of the matrix element of a creation operator between initial and final states and  $C$  is the isospin Clebsch-Gordan coefficient. In a schematic form, between basis states for  $n$  particles in a shell,

$$\langle n ||| a^\dagger ||| n-1 \rangle = \sqrt{n} \langle n-1, 1 | \} n \rangle \quad (3)$$

where the coefficients of fractional parentage (cfp's) are products of weight factors and Clebsch-Gordan coefficients for  $SU(3) \supset O(3)$  and  $SU(4) \supset SU(2) \times SU(2)$  [48]. The weight factors  $\sqrt{\frac{n_{f'}}{n_f}}$  are particularly important because they give the branching to states of final symmetry  $[f']$  which can be reached from an initial symmetry  $[f]$ . If more than one  $[f']$  is allowed, there will be parentage to widely separated states of the  $A - 1$  core nucleus. For example, for  $A = 13$  the weights for  $[441] \rightarrow [44]$  and  $[431]$  are  $\sqrt{\frac{1}{4}}$  and  $\sqrt{\frac{3}{4}}$ , respectively. On the other hand, nucleon removal from  $^{12}\text{C}$  leads only to the  $\frac{3}{2}_1^-$ ,  $\frac{1}{2}_1^-$ , and  $\frac{3}{2}_2^-$  states of  $^{11}\text{C}$  or  $^{11}\text{B}$  because  $[44] \rightarrow [43]$  is the only possibility. For  $N > Z$ , the sum rule  $\sum C^2 S(T_>) = Z$  applies for proton removal, with the  $T_>$  states generally belonging to a different  $[f']$  from the  $T_<$  states, while both  $T_<$  and  $T_>$  states contribute for neutron removal.

It is very easy to generate spectroscopic amplitudes for multinucleon transfer from the one-particle cfp's of Eq. (3). For 3 and 4 nucleon removal, it is assumed that the  $k$  nucleons have maximum spatial symmetry  $[k]$ , which can be projected onto a  $(0s)^k$  internal wave function for the cluster. Amplitudes for 1 - 4 nucleon transfer have been tabulated [49] for the Cohen and Kurath wave functions. The generalization to other major shells and mixed major shells is straightforward.

### 3.2 The He isotopes

There is now considerable evidence for a number of relatively narrow excited states in  $^{8-10}\text{He}$  [18]. The positions of the lowest narrow states in  $^9\text{He}$  and  $^{10}\text{He}$  are consistent with the p-shell expectations of Ref. [50] and this work. The widths of  $^5\text{He}(\frac{3}{2}_1^-)$ ,  $^7\text{He}(\frac{3}{2}_1^-)$ , and  $^8\text{He}(2_1^+)$  calculated according to Eq. (2) are in good agreement with the experimental values. However, the nominally  $p_{1/2}$  state ( $S(th) = 0.65 - 0.83$ ) at 1.13 - 1.27 MeV above threshold in  $^9\text{He}$  [18] is predicted to have a width in excess of 1 MeV, which more than a factor of 2 larger than is reported. Very recently, strong evidence has been obtained that the ground state of  $^9\text{He}$  is an unbound s-state with a scattering length of  $\leq -10$  fm [51]. The WBP and WBT interactions [24] predict that the  $\frac{1}{2}^+$  state should be lowest [51] followed by a  $\frac{1}{2}^-$  state, and a  $\frac{5}{2}^+$ ,  $\frac{3}{2}^-$  pair 2.2 and 2.4 MeV above the  $\frac{1}{2}^+$  state; Poppelier et al. make very similar predictions [52]. The  $\frac{5}{2}^+$  state could correspond to the second state seen in the  $^9\text{Be}(^{14}\text{C}, ^{14}\text{O})^9\text{He}$  reaction [18] at  $E_n = -S_n \sim 2.4$  MeV ( $\Gamma_d^{sp} = 624$  keV). In any case, transfer reactions of this type should populate a number of narrow states of the form  $^8\text{He}(0^+, 2^+) \otimes (sd)$ . The presence of the low-lying sd states in  $^9\text{He}$  clearly has implications for the structure of  $^{10}\text{He}$ .

Recently, an excited state of  $^7\text{He}$  which decays mainly into the  $^4\text{He} + 3n$  channel

has been observed via the  $p(^8\text{He}, d)^7\text{He}$  reaction [53] at  $E_x = 2.9(3)$  MeV with  $\Gamma = 2.2(3)$  MeV. The p-shell  $\frac{5}{2}^-$  state, which is predicted slightly higher in energy, has the correct decay properties but must be produced via a two-step process [53]. Also, a broad state at  $\sim 3.2$  MeV is seen in the  $^9\text{Be}(^{15}\text{N}, ^{17}\text{F})^7\text{He}$  reaction and assigned  $J^\pi = \frac{1}{2}^-$  [54]. However, a  $\frac{1}{2}^-$  state at this energy would be exceedingly broad and, in addition, the calculated spectroscopic factor for two-proton pickup from  $^9\text{Be}$  is vanishingly small. The  $\frac{5}{2}^-$  state, on the other hand, has a substantial  $L=2, S=0$  two-proton spectroscopic factor.

### 3.3 The Li isotopes

There have been many investigations of the unbound nucleus  $^{10}\text{Li}$ . These are summarized in recent works which confirm the existence of s-wave strength near threshold [55] and a p-wave resonance at 500 keV above threshold with a width of 400(60) keV [56]. Shell-model calculations predict a low-lying  $1^+, 2^+$  doublet separated by only 23 keV for the  $A = 10-12$  interaction (and 169 keV for the  $A = 6-9$  interaction) with  $S = 0.98$  and  $0.71$ , respectively. At  $E_n = 500$  keV, the predicted width for the  $1^+$  state is 375 keV; a slightly narrower, nearly degenerate  $2^+$  state could also be populated in the experiments. The  $^{10}\text{Be}(^{12}\text{C}, ^{12}\text{N})^{10}\text{Li}$  reaction shows evidence for states at  $E_n = 0.24, 1.40,$  and  $4.19$  MeV [18].

Based on the evidence from  $^{10}\text{Li}$  and general systematics, states of the form  $^9\text{Li}(0\hbar\omega) \otimes (sd)^2$  and  $^{10}\text{Li}(0\hbar\omega) \otimes (sd)$  are expected close in energy to the simple p-shell  $\frac{3}{2}^-$  configuration for  $^{11}\text{Li}$ . Indeed, the interactions of Warburton and Brown [24] predict essential degeneracy of the lowest  $0\hbar\omega$  and  $2\hbar\omega$  configurations in  $^{11}\text{Li}$  (and  $^{12}\text{Be}$ ). The evidence from  $^{11}\text{Li}$   $\beta$  decay for strong mixing has already been mentioned and an analysis of a fragmentation experiment [57] comes to the same conclusion. There is also evidence for a number of relatively narrow excited states [18] which are necessarily not of p-shell origin and must be explained by any realistic structure calculation.

### 3.4 The Be isotopes

Many years ago, Kurath and Pičman [58] showed that the lowest p-shell states generated using a central plus one-body spin-orbit interaction had an essentially perfect overlap with states projected from a Slater determinant of the lowest Nilsson orbits for a Nilsson Hamiltonian with the same spin-orbit interaction as the shell model and a deformation that varied in a very regular way throughout the p-shell. In cases where two bands with different  $K$  lie close together, linear combinations of the two  $J$ -projected states reproduce



the two corresponding shell-model states. In Elliott's SU(3) model [11], states with good orbital angular momentum are obtained by projection from a Slater determinant, or linear combination thereof, of asymptotic Nilsson orbits. In the case of non-zero intrinsic spin, Elliott and Wilsdon [59] projected states with good  $J$  and  $K_J = K_L + K_S$  from a product of the SU(3) intrinsic state and the intrinsic spin wave function. The  $J$ -projected states correspond to a well-defined linear combination of  $L$ -projected LS-coupling states. In the shell model, the spin-orbit interaction drives the mixture of states with different  $L$ . Of course, the spin-orbit interaction also mixes different SU(3) representations through its (1 1) tensor character. In the supermultiplet, or SU(3), basis it is very easy to see the band structure and to check the degree to which  $K_J$  is a good quantum number.

The first  $K = \frac{1}{2}$  orbit for prolate deformation is filled at  ${}^8\text{Be}$  and the interplay of the remaining  $K = \frac{3}{2}$  and  $K = \frac{1}{2}$  orbits can be seen beyond  $A = 8$ .  ${}^9\text{Be}$  has a  $K = \frac{3}{2}$  ground-state band with  $L = 1$  and  $L = 2$  in the ratio  $\sqrt{\frac{21}{26}}$  to  $-\sqrt{\frac{5}{26}}$  in the SU(3) limit (the same is true for  ${}^{11}\text{B}$ ). For  $A = 10$ , two particles in the  $K = \frac{3}{2}$  orbit give rise to the  $K = 3$  ground-state band of  ${}^{10}\text{B}$  for  $T = 0$  ( $S = 1$ ) and to the  $K = 0$  ground-state band of  ${}^{10}\text{Be}$  for  $T = 1$  ( $S = 0$ ). In the latter case, promoting one neutron to the next  $K = \frac{1}{2}$  orbit gives the  $K = 2$  bandhead at 5.958 MeV, as shown in Fig. 2. The reason for the very strong population of this state via a Gamow-Teller transition in the (t,  ${}^3\text{He}$ ) reaction on  ${}^{10}\text{B}$  [60] can be seen from the  $L$  decomposition of the pure  $K_L = 2$ ,  $K_S = 1$   ${}^{10}\text{B}$  ground state,

$$|{}^{10}\text{B } 3^+ K_J = 3\rangle = \sqrt{\frac{6}{7}}|L = 2\rangle - \sqrt{\frac{3}{22}}|L = 3\rangle + \sqrt{\frac{1}{154}}|L = 4\rangle ,$$

as can the reason for the excitation of the  $K_L = 2$ ,  $3^+$  state at 9.40 MeV. The 3.37-MeV  $2^+$  state is seen weakly, some  $K$  mixing of the  $2^+$  states being necessary to ensure the near equality of the  $2_1^+ \rightarrow 0^+$  E2 (isoscalar) transitions in  ${}^{10}\text{Be}$  and  ${}^{10}\text{C}$  [13]. The  $2^+$  state near 9.6 MeV in Fig. 2 is seen in proton pickup from  ${}^{11}\text{B}$  [13] and corresponds to a p-shell state with [33] symmetry. States with [411] symmetry are also predicted near 10 MeV but they would have very large neutron decay widths. The near degeneracy of the  $1\hbar\omega$  and  $2\hbar\omega$  configurations has long been known [13] and is nicely reproduced in a number of recent cluster model calculations [26–28].

For the last three neutrons in  ${}^{11}\text{Be}$ , one expects bands formed from  $(K = \frac{3}{2})^2$  ( $K = \frac{1}{2}$ ) and  $(K = \frac{3}{2})(K = \frac{1}{2})^2$  intrinsic states. In the shell-model the corresponding bands in the SU(3) limit have  $(\lambda \mu) = (2 1)$  ([421] spatial symmetry) with  $K_L = 1$  and  $K_S = \pm\frac{1}{2}$ ; the details are shown in Table 1, where it can be seen that the wave functions are indeed dominantly of [421] symmetry with  $K = \frac{1}{2}$ . With respect to identifying experimental candidates for these states,

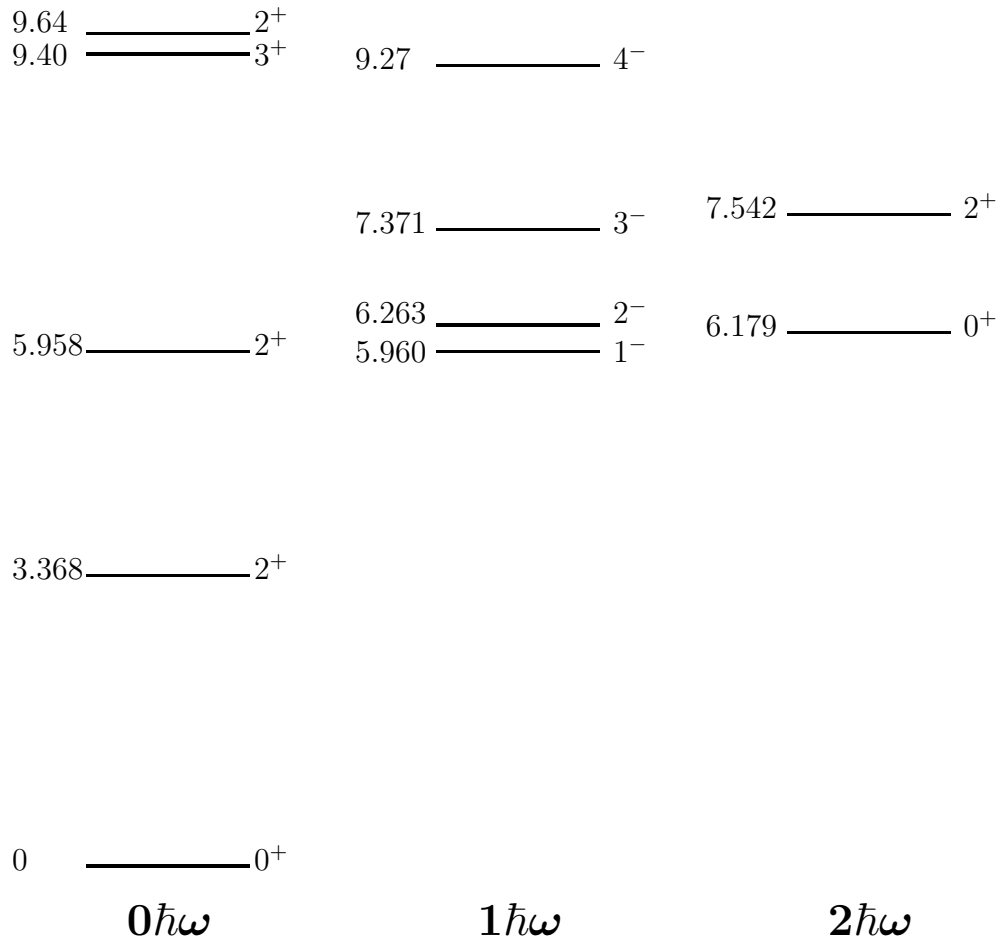


Fig. 2. States of  $^{10}\text{Be}$  below 10 MeV excitation energy.

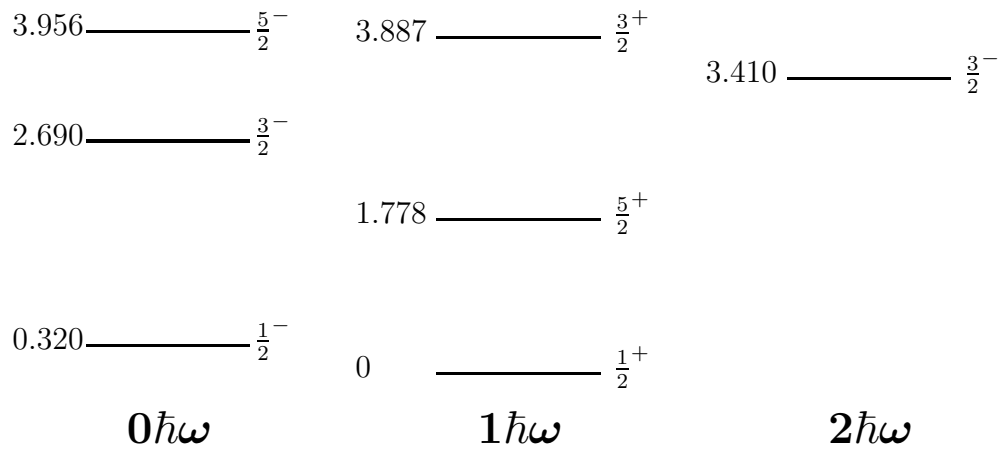


Fig. 3. States of  $^{11}\text{Be}$  below 4 MeV excitation energy.

Table 1

States in the p-shell  $K = \frac{1}{2}$  band of  $^{11}\text{Be}$  with the bandhead at 0.320 MeV for the fitted  $A = 10 - 12$  interaction.

$J^\pi$	$E_x$	Pure [421] wave function	% [421]	% [421] $K = \frac{1}{2}$
$\frac{1}{2}^-$	0.32	$ L = 1\rangle$	93	93
$\frac{3}{2}^-$	2.66	$\sqrt{\frac{2}{5}} L = 1\rangle + \sqrt{\frac{3}{5}} L = 2\rangle$	79	76
$\frac{5}{2}^-$	3.63	$\sqrt{\frac{7}{15}} L = 2\rangle + \sqrt{\frac{8}{15}} L = 3\rangle$	80	79

the tabulation [61] is misleading since the spin and parity assignments are based on  $(t, p)$  angular distributions contradicted by later work [62]. Pickup reactions from heavier p-shell nuclei provide a clean way to identify dominantly p-shell states. In the  $^{13}\text{C}(^6\text{Li}, ^8\text{B})^{11}\text{Be}$  reaction [63], the  $\frac{1}{2}^-$  state and states at 2.69 MeV and 4.0 MeV are seen. Also, four  $T = \frac{3}{2}$  states in  $^{11}\text{B}$  have been identified via the  $^{14}\text{C}(p, \alpha)^{11}\text{B}$  reaction [64], the first three of which were identified with first  $\frac{1}{2}^-$ ,  $\frac{3}{2}^-$ , and  $\frac{5}{2}^-$  states, the latter two at 2.37 MeV and 3.58 MeV relative to the first. The shell-model spectroscopic amplitudes are consistent with the assignments from these two reactions. The strong branch to 2.69-MeV level in the  $\beta$  decay of  $^{11}\text{Li}$  [44] is model-independent evidence of negative parity for this level.

The level scheme for states below 4 MeV shown in Fig. 3 is the same as that from Liu and Fortune's analysis of the  $^9\text{Be}(t, p)^{11}\text{Be}$  reaction [62] with the exception of the 3.956-MeV level. However, the  $L = 2$  angular distribution observed for this level is consistent with a  $\frac{5}{2}^-$  assignment and the discussion in the previous paragraph indicates that one of the two levels in this region is the first p-shell  $\frac{5}{2}^-$  level. Charge-exchange reactions also see strength in this region [60]. The ratios of strengths to the 0.32 and 2.69 levels, and to the 3.9 MeV region in  $^{11}\text{Li}(\beta^-)$  decay [44] is consistent with the shell-model prediction although there is some uncertainty over the the division of strength between the 3.89 and 3.96 MeV levels. The authors of Ref. [44] favour an interchange of the  $\frac{3}{2}^-$  and  $\frac{3}{2}^+$  assignments for the 3.41 and 3.89 MeV levels in Fig. 3. However, the width of the 3.41 MeV level is over 100 keV [62] and this is inconsistent with the small  $d_{3/2}$  spectroscopic predicted for the lowest  $\frac{3}{2}^+$  level and the calculated d-wave single-particle width of 144 keV. The predicted width for the p-shell  $\frac{5}{2}^-$  level at 3.96 MeV is 17 keV for  $S(2^+) = 0.66$  compared with the experimental value of 15(5) keV; a slightly smaller value  $S(2^+) = 0.49$  is required to give the observed width of 201(10) keV for the apparent analog in  $^{11}\text{B}$ .

All three states of the  $K^\pi = \frac{1}{2}^-$  band have large parentages for neutron removal from  $^{12}\text{N}$ . The proton spectrum which results from the decay of the resulting  $^{11}\text{N}$  states has been studied [65] and can be qualitatively reproduced using the calculated decay widths for the p-shell states of  $^{11}\text{N}$ .

An important point is that the parentage for neutron removal from the [421] symmetry p-shell states is complex because the parentage to the allowed symmetries [42], [411], and [321] is divided in the ratio 9:10:16. The model independent sum rules for  $S(T_<)$  and  $S(T_>)$  are 4.5 and 2.5. Of the  $C^2S = 5$  for neutrons, 0.5 must go to  $T = 2$  states at  $\sim 22$  MeV excitation energy in  $^{10}\text{Be}$ , 1.8 to [42] states, and 2.0 to [411] states. For the lowest  $\frac{1}{2}^-$  state, about 2.2 of the parentage goes to the ground state and the first two  $2^+$  states and about 1.6 to states in the 9–13 MeV energy range, so that there is a small redistribution of strength from the pure symmetry limit. This parentage is necessary for a properly antisymmetric  $\frac{1}{2}^-$  wave function so that one should be suspicious of particle-core coupling models for the  $\frac{1}{2}^-$  state which include only the lowest  $0^+$  and  $2^+$  core states. In fact, the shell-model parentage is considerably larger to the second  $2^+$  state than to the first, as one might guess from the Nilsson model picture of the states involved; the spectroscopic factors for the  $0_1^+$ ,  $2_1^+$ , and  $2_2^+$  states of the core are 0.75, 0.45 and 1.00 (0.63, 0.65, and 0.93 for the (8-16)2BME interaction of Cohen and Kurath [38]). In contrast the parentage for the  $\frac{1}{2}^+$  ground state of  $^{11}\text{Be}$  is mainly to the first  $0^+$  and  $2^+$  states with  $K_L = 0$ .

That many of the known states of  $^{12}\text{Be}$  are mainly of  $(sd)^2$  character was suggested long ago and is rather obvious from an analysis of  $^{10}\text{Be}(t, p)$  data and the resultant comparison with known  $(sd)^2$  states in  $^{14}\text{C}$  and  $^{16}\text{C}$  [66]. For  $^{13}\text{Be}$  and  $^{14}\text{Be}$ , neutrons have to occupy sd orbits.

#### 4 Non-normal parity states in the p-shell

States with a nominal  $1\hbar\omega$  excitation energy are formed by  $0s \rightarrow 0p$  and  $0p \rightarrow 1s0d$  excitations with both configurations usually being present to prevent unphysical centre-of-mass excitations but with the latter dominating at low excitation energies. One interaction that has been widely used one due to Millener-Kurath (MK) developed for a study of the  $\beta$  decay of  $^{14}\text{B}$  [67]. The MK interaction was “hand crafted” to give a good account of the relative separation of the  $1s_{1/2}$  and  $0d_{5/2}$  centroids as a function of mass number, through  $^{13}\text{C}$  and down to  $^{11}\text{Be}$ . More attention was given to  $A = 11$  by Teeters and Kurath [68] and by Millener and collaborators in studies of the the  $\beta$  decay of  $^{11}\text{Be}$  [69] and the fast E1 transition in  $^{11}\text{Be}$  [70]. Warburton and Brown [24] have subsequently shown that it is possible to obtain a successful fit with an rms deviation of  $\sim 330$  keV to a large number of cross-shell energies from  $A = 10 - 22$ , including some for  $2\hbar\omega$  configurations.

The lowering of the  $1s_{1/2}$  orbit with respect to the  $0d_{5/2}$  orbit is expected for a simple potential well. In shell-model calculations it arises because in the potential energy contributions to the single-particle energies at  $^{17}\text{O}$ , the  $0d_{5/2}$

nucleon interacts more strongly with the  $0p$  nucleons while the  $1s_{1/2}$  nucleon interacts more strongly with the  $0s$  nucleons. The sum of the interactions with both shells of the core is similar at  $^{17}\text{O}$  but the  $0d$  orbit loses attraction relative to the  $1s$  orbit as p-shell nucleons are removed. In fact, half the difference between the interactions with the full p shell roughly accounts for the 2.65 MeV shift in the relative  $\frac{1}{2}^+$ ,  $\frac{5}{2}^+$  separation between  $^{17}\text{O}$  and  $^{11}\text{Be}$ . The shift between  $^{17}\text{O}$  and  $^{15}\text{C}$  is related simply to the properties of the  $T=1$   $p_{1/2}^{-1}d_{5/2}$  and  $p_{1/2}^{-1}s_{1/2}$  interactions which may be read directly from the spectrum of  $^{16}\text{N}$  [10]. These four particle-hole matrix elements control the basic energetics of all the heavy carbon and nitrogen isotopes (see Section 5).

Table 2 shows the systematics of energies with respect to neutron thresholds, ‘‘Coulomb energies’’, decay widths, and dominant weak-coupling components of the proton-rich members of isospin multiplets for  $1\hbar\omega$  states from  $A = 11 - 17$  (one exception is that for  $A = 14$  the widths are given for  $^{14}\text{N}$  because of the paucity of information, apart from the  $1^-$  state, for  $^{14}\text{O}$ ). All the states have isospin  $T = T_c + \frac{1}{2}$ ; states with lower isospin gain considerable binding energy because a higher spatial symmetry is possible. Because the sd-shell nucleon is not restricted by the Pauli Principle, the neutron separation energies show a rather smooth variation with mass number (third column of Table Table 2), in analogy with the classic example of  $\Lambda$  separation energies [71]. The separation energy eventually has to cross zero as the mass number decreases. At the same time, the separation energy for a p-shell neutron is going towards zero as neutrons are added so that there is inevitably competition between (at least)  $0\hbar\omega$ ,  $1\hbar\omega$ , and  $2\hbar\omega$  configurations. The energies of the lowest  $(A - 2) \otimes \nu(sd)^2(0^+)$  states relative to the two-neutron separation threshold also show a very smooth behaviour, with approximately constant values along isotopic chains; e.g., (6.53, 6.69, 5.47) MeV for  $^{14-16}\text{C}$ , (4.54, 4.57, 3.74) MeV for  $^{13-15}\text{B}$ , and (2.30, 3.91, 3.67) MeV for  $^{10-12}\text{Be}$ .

The Coulomb energies given in Table 2 are not true Coulomb energy differences except for  $T = \frac{1}{2}$ . Rather they reflect the differences between neutron and proton separation energies at either end of the isospin multiplet. The calculated  $\Delta E_C^{th}$  for a pure weak-coupling configuration involves choosing the well depth for a Woods-Saxon well of standard geometry to fit the neutron separation energy, then turning on the Coulomb potential of a uniformly charged sphere and computing the proton separation for  $N$  and  $Z$  interchanged. For mixed configurations, the calculated  $\Delta E_C^{th}$  are weighted by the shell-model parent-ages, enabling the binding energy of the proton-rich member to be estimated.

To take the example of the  $^{11}\text{Be}$ ,  $^{11}\text{N}$  pair,  $\Delta E_C^{sp}$  is 1.58 MeV for a pure  $1s_{1/2}$  configuration and 2.92 MeV for a  $2_1^+ \otimes d_{5/2}$  configuration (15% of the shell-model wave function).  $\Delta E_C^{sp}$  is slightly higher still for the remaining 4% of the shell-model wave function. Performing the average puts the  $^{11}\text{N}$  ground state 1.34 MeV above the  $^{10}\text{C} + p$  threshold. This can be compared with a recent

Table 2

Observed and calculated Coulomb energy shifts and nucleon decay widths for  $1\hbar\omega$  states which have dominantly  $1s_{1/2}$  or  $0d_{5/2}$  character. The trend with changes in binding energy is made clearer by normalizing all  $\Delta E_C$  to a  $Z_> = 6$  core.

Nucleus	$J^\pi$	$E_n$	$\Delta E_C^{th}$	$\Delta E_C^{exp}$	$\Gamma^{th}$	$\Gamma^{exp}$	Comments
$^{11}\text{Be}$	$\frac{1}{2}^+$	-0.503	1.845	1.773	1467	1440(200)	81% $s_{1/2}(gs)$
$^{12}\text{B}$	$2^-$	-1.696	2.309	2.286	87	118(14)	70% $s_{1/2}(gs)$
	$1^-$	-0.749	1.942	1.948	894	750(250)	76% $s_{1/2}(gs)$
	$1^-$	-1.194	2.046	$\sim 2.09$	311	260(30)	77% $s_{1/2}(\frac{1}{2}^-)$
$^{13}\text{C}$	$\frac{1}{2}^+$	-1.857	2.238	2.278	32	31.7(8)	89% $s_{1/2}(gs)$
	$\frac{3}{2}^+$	-1.699	2.189	2.205	84	115(5)	87% $s_{1/2}(2^+)$
	$\frac{5}{2}_2^+$	-2.521	2.437	2.502	7	11	74% $s_{1/2}(2^+)$
$^{14}\text{C}$	$1^-$	-2.083	2.280	2.252	28.8	30(1)	76% $s_{1/2}(gs)$
$^{15}\text{C}$	$\frac{1}{2}^+$	-1.218	1.857	2.016	934	1000(200)	98% $s_{1/2}(gs)$
$^{16}\text{N}$	$0^-$	-2.371	2.168	2.180	21	40(20)	100% $s_{1/2}(gs)$
$^{16}\text{N}$	$1^-$	-2.094	2.113	2.117	78	< 40	97% $s_{1/2}(gs)$
$^{17}\text{O}$	$\frac{1}{2}^+$	-3.273	2.301	2.376			100% $s_{1/2}(gs)$
$^{11}\text{Be}$	$\frac{5}{2}^+$	1.275	2.520	2.475	535	600(50)	67% $d_{5/2}(gs)$
$^{12}\text{B}$	$3^-$	0.019	2.543	2.512	220	220(25)	88% $d_{5/2}(gs)$
	$4^-$	1.148	2.519	$\sim 2.66$	610	744(25)	82% $d_{5/2}(gs)$
	$3^-$	0.231	2.505	2.516	280	180(23)	70% $d_{5/2}(\frac{1}{2}^-)$
$^{13}\text{C}$	$\frac{9}{2}^+$	0.115	2.526	2.503	258	280(30)	91% $d_{5/2}(2^+)$
	$\frac{7}{2}^+$	-1.892	2.731	2.666	3	9.0(5)	92% $d_{5/2}(2^+)$
	$\frac{5}{2}^+$	-1.093	2.675	2.695	45	47(7)	80% $d_{5/2}(gs)$
$^{14}\text{C}$	$3^-$	-1.449	2.636	2.651	13.4	16(2)	84% $d_{5/2}(gs)$
	$2^-$	-0.836	2.615	2.570	38.2	41(2)	66% $d_{5/2}(gs)$
$^{15}\text{C}$	$\frac{5}{2}^+$	-0.478	2.446	2.436	222	240(30)	93% $d_{5/2}(gs)$
$^{16}\text{N}$	$2^-$	-2.491	2.609	2.588	3.5	40(30)	96% $d_{5/2}(gs)$
$^{16}\text{N}$	$3^-$	-2.193	2.585	2.587	12	< 15	96% $d_{5/2}(gs)$
$^{17}\text{O}$	$\frac{5}{2}^+$	-4.144	2.609	2.658			100% $d_{5/2}(gs)$

result of  $1.27_{-0.05}^{+0.18}$  MeV from resonance elastic scattering of protons [72] (see also a result from transfer reactions [73]). Although the complex resonance energy is close to becoming unstable, the computed width in Table 2 is close to the value of 1.44(20) MeV from the same experiment. All in all, Table 2 shows remarkable agreement with experiment for both energies and widths even in the case of broad states. Encouraged by the similarity in structure and separation energy for  $^{12}\text{N}(1_1^-)$  and  $^{11}\text{N}(\frac{1}{2}^+)$ , one could also extrapolate the experimental energies in Table 2 for low  $1s_{1/2}$  neutron binding energy to make a reliable estimate for the  $^{11}\text{N}$  ground state energy.

The differences in Coulomb energies for the  $0p$ ,  $1s$ , and  $0d$  orbits, which are considerable, and their behaviour as a function of binding provide a very sensitive tests of the structure of nuclear states. The well-known Nolan-Schiffer anomaly for Coulomb energies can be bypassed by taking only direct Coulomb energies [74] with an overall energy scale set by the radius parameter of the single-particle well, as has been done in Table 2. The agreement with experiment suggests that the shell-model parentages are realistic, including the case of  $^{11}\text{Be}$  over which there has been much debate. A recent measurement of  $\mu = -1.6816(8)\mu_N$  for the magnetic moment of  $^{11}\text{Be}$  [75], which is sensitive to the  $2^+ \otimes d_{5/2}$  admixture [76], tends to confirm the MK parentage which gives  $\mu = -1.71\mu_N$  when bare-nucleon g-factors are used. Note that Suzuki et al. [76] used a quenched spin g-factor based on the tabulated value of  $\mu = -1.315(70)\mu_N$  for  $^{15}\text{C}$ . However, this value appears only in a conference proceedings and I strongly suspect that it is not correct; based on the parentage for  $^{15}\text{C}$  ground states in Table 2,  $\mu(^{15}\text{C})$  should be closer to the Schmidt value than  $\mu(^{11}\text{Be})$ .

Recent experiments come to the same conclusion about the parentage of the  $^{11}\text{Be}$  ground state. Analysis of the one-neutron knockout reaction with coincident detection of  $\gamma$  rays from the  $^{10}\text{Be}$  core [77] determines that the ground-state spectroscopic factor of 0.74 from the WBP interaction [24] is consistent with the data; the slightly higher value from the MK interaction would give even better agreement. Likewise, analysis of the  $^{11}\text{Be}(p,d)^{10}\text{Be}$  reaction in inverse kinematics leads to a  $2^+ \otimes d_{5/2}$  admixture of  $\sim 16\%$  [78].

In the one-nucleon knockout reaction ( $^{12}\text{Be}, ^{11}\text{Be} + \gamma$ ) reaction on a  $^9\text{Be}$  target [23], comparable spectroscopic factors are extracted for the bound  $\frac{1}{2}^+$  and  $\frac{1}{2}^-$  states of  $^{11}\text{Be}$  explicitly demonstrating the breakdown of the  $N = 8$  shell closure. The shell-model calculations using the WBP interaction [24] reproduce the data quite well. They also predict substantial parentage to the unbound  $\frac{5}{2}^+$  state of  $^{11}\text{Be}$  [23]. The latter parentage is a warning of the inadequacy, over and above center of mass problems, of calculations which limit the number of  $sd$  orbits to the  $1s_{1/2}$  orbit. Even the  $d_{3/2}^2$  configuration is important because of a large matrix element with  $d_{5/2}^2$ . Proton removal from  $^{13}\text{B}$  would provide another way to study the mixing of  $0\hbar\omega$  and  $2\hbar\omega$   $0^+$  and  $2^+$  states in  $^{12}\text{Be}$ ,

the predicted  $C^2S$  values for pickup to the lowest p-shell  $0^+$  and  $2^+$  being 0.52 and 2.12, respectively. Also in  $^{12}\text{Be}$ , a  $1^-$  state has been seen at 2.68(3) MeV by observing  $\gamma$  rays following the inelastic scattering of  $^{12}\text{Be}$  on a lead target [79].

The parentage of  $^{13}\text{Be}$  and  $^{14}\text{Be}$  to  $^{12}\text{Be}$  is clearly complicated by the fact that  $(sd)^2$  configurations form a substantial component of low-lying states in  $^{12}\text{Be}$ . A state in  $^{13}\text{Be}$  with probable  $d_{5/2}$  parentage to  $^{12}\text{Be}$  has been located 2.0 MeV above the neutron threshold [80]; both  $p^8(sd)$  and  $p^6(sd)^3$  configurations probably need to be considered. A number of other states have also been seen [80,81] including a possible ground state 0.78 MeV above threshold with  $^{11}\text{Be}(\frac{1}{2}_1^-) \otimes (sd)^2$  as the most likely candidate.

## 5 The heavy boron, carbon, and nitrogen isotopes

From the discussion in the previous section, it is clear that the “stretched isospin” wave functions for a p-shell core plus neutrons in the sd shell can usually be described in terms of a few dominant weak-coupling components involving low-lying states of the core. The same is true for cases involving p-shell proton holes and sd-shell neutrons because then only the weak and repulsive  $T = 1$  particle-hole interaction acts. For the nitrogen and carbon isotopes one can assume to a first approximation that the lowest states are formed by coupling the  $^{15}\text{N}$  or  $^{14}\text{C}$  ground state to states of the appropriate oxygen isotope. For  $p^{-m}(sd)^n$  configurations, an estimate of the mass excess can be obtained from

$$ME(A) = ME(16 - m) + ME(16 + n) - ME(^{16}\text{O}) + \langle V_{ph} \rangle, \quad (4)$$

where the  $ME$  denote experimental mass excesses and  $\langle V_{ph} \rangle$  is a weighted average of  $mn$  particle-hole interactions, dominated by the  $p_{1/2}^{-1}d_{5/2}$  and  $p_{1/2}^{-1}s_{1/2}$  interactions, which can be taken from  $^{16}\text{N}$ . For a simple monopole interaction of the form  $a + bt_p.t_h$ ,  $\langle V_{ph} \rangle = mn(a + b/4)$  and the fact that an essentially constant value for  $a + b/4$  can be extracted from any of the known heavy C or N isotopes demonstrates the basic consistency of the approximation. Of course there is mixing in a shell-model calculation, a good example being the importance of small  $p_{3/2}^{-1}$  admixtures for  $\mu(^{18}\text{N}(1^-))$ , for which two discordant results have been reported [82].

Two recent experimental studies involving one-neutron removal reactions have used wave functions based on the WBP interaction [24] in their analysis. The first is a systematic study on 23 neutron-rich psd-shell nuclei with  $Z = 5 - 9$  and  $A = 12 - 25$  [83] and the second, with coincident  $\gamma$ -ray detection, is a



study of  $^{16,17,19}\text{C}$  [84]. In the latter work, the ground-state spins of  $^{17}\text{C}$  and  $^{19}\text{C}$  are assigned as  $\frac{3}{2}^+$  and  $\frac{1}{2}^+$  respectively. This means that the particle-hole interaction inverts the order of the  $^{19}\text{O}$  ground-state doublet in  $^{17}\text{C}$  but does not lower the configuration involving the 1.472-MeV  $\frac{1}{2}^+$  state of  $^{19}\text{O}$  enough to become the ground state of  $^{17}\text{C}$ . However, the converse is true in  $^{19}\text{C}$  for the configuration involving the 1.33-MeV  $\frac{1}{2}^+$  state of  $^{21}\text{O}$ .

In the case of the boron isotopes, particle-hole interactions involving a  $p_{3/2}$  hole necessarily play an important role. The tabulations [13] show no definite spin-parity assignments for excited states of the core nucleus  $^{13}\text{B}$ . Recently, spins of  $\frac{3}{2}^+$  and  $\frac{5}{2}^+$  have been suggested for the 3.48 and 3.68 MeV states on the basis of a one-neutron knockout experiment [85]. In addition, a wealth of new information has been obtained on states of  $^{13-16}\text{B}$  using multinucleon transfer reactions [86]. For example, the strongest state in one-proton removal, two-neutron addition reactions on  $^{12}\text{C}$  leading to  $^{13}\text{B}$  is a state at 6.42 MeV. This state almost certainly corresponds to the  $\frac{9}{2}^+$   $\text{T}=\frac{3}{2}$  state at 21.47 MeV in  $^{13}\text{C}$  which is strongly excited by an M4 transition in inelastic electron scattering. The predicted width for the  $^{12}\text{B}(2^+) \otimes \nu d_{5/2}$  analog in  $^{13}\text{B}$  is 33 keV, which is in excellent agreement with the tabulated width of 36(5) keV. Measurements have also been made for the ground-state moments of a number of the boron isotopes and successfully interpreted in terms of shell-model calculations [87].

## 6 Discussion

The structure of neutron-rich light nuclei has been discussed in terms of shell-model calculations that include all configurations at a given  $n\hbar\omega$  level of excitation. Other models which can better take into account the radial degrees of freedom necessary to describe loose binding and clustering effects tend to be applied to specific cases rather than to describe the broad systematics of nuclear spectra. In any case, the results of these calculations are usually interpreted in terms of the essential shell-model configurations involved.

The major question that has to be addressed in any calculation is how to treat the mixing of configurations which differ in energy by  $2\hbar\omega$  or more. Certainly, if only the lowest few states of each diagonalized  $n\hbar\omega$  space are kept and mixed in what might be called an extended coexistence model, good spectra and a good description of the relationships (parentage) between low-lying states in neighbouring nuclei can be achieved. This has been the approach in a number of the cluster-model calculations referenced earlier.

The shell-model runs into consistency problems if diagonalizations are performed in complete  $(0+2)\hbar\omega$  spaces rather than using the ‘‘coexistence’’ approach [88,89,24]. The crux of the matter is that the dominant  $\Delta\hbar\omega = 2$

interaction transforms as a (20) SU(3) tensor (just as most of  $H$  in Eq. (1) transforms as (00) for  $\Delta\hbar\omega = 0$ ) leading to large matrix elements between quite widely separated configurations and slow convergence as a function of  $\hbar\omega$ . Powerful mathematical techniques exist for the symplectic shell model, a natural extension of Elliott's SU(3) model, and the cluster model to handle calculations in "vertically" truncated model spaces (see articles in Ref. [40]). The correlations induced in low-energy wave functions can be viewed both as improvements to the radial wave functions between clusters and as an introduction of the RPA-type correlations necessary to satisfy energy-weighted sum rules.

## Acknowledgements

This work was supported by the US Department of Energy under Contract No. DE-AC02-98-CH10886 with Brookhaven National Laboratory. I would like to thank B. Alex Brown for many interesting discussions.

## References

- [1] Proceedings of the International Conference on Nuclear Structure, Kingston, Canada, Eds. D.A. Bromley and E.W. Vogt (University of Toronto Press, 1960).
- [2] D.H. Wilkinson, *Annu. Rev. Nucl. Part. Sci.* **45** (1995) 1.
- [3] J.P. Elliott and A.M. Lane, *Encyclopedia of Physics*, ed. S. Flügge (Springer-Verlag, 1957), p. 241.
- [4] J.P. Elliott and B.H. Flowers, *Proc. Roy. Soc.* **A229** (1955) 536.
- [5] D. Kurath, *Phys. Rev.* **101** (1956) 216.
- [6] J.P. Elliott and B.H. Flowers, *Proc. Roy. Soc.* **A242** (1957) 57.
- [7] R.F. Christy and W.A. Fowler, *Phys. Rev.* **96** (1954) 851.
- [8] A.M. Lane, *Proc. Phys. Soc. A* **66** (1954) 977.
- [9] D.H. Wilkinson and D.E. Alburger, *Phys. Rev.* **113** (1959) 563.
- [10] I. Talmi and I. Unna, *Phys. Rev. Lett.* **4** (1960) 469.
- [11] J.P. Elliott, *Proc. Roy. Soc. A* **245** (1958) 128, 562; *J. Phys. G* **25** (1999) 577.
- [12] F. Ajzenberg-Selove and T. Lauritsen, *Nucl. Phys.* **11** (1959) 1.
- [13] <http://www.tunl.duke.edu/nucldata>

- [14] ENAM98, Eds. B.M. Sherrill, D.J. Morrissey, and C.N. Davids, AIP Conference Proceedings **455** (AIP, Woodbury, New York, 1998).
- [15] A.C. Mueller and B.M. Sherrill, Annu. Rev. Nucl. Part. Sci. **43** (1993) 529.
- [16] P.G. Hansen, A.S. Jensen, and B. Jonson, Annu. Rev. Nucl. Part. Sci. **45** (1995) 591.
- [17] I. Tanihata, J. Phys. G **22** (1996) 157; Nucl. Phys. **A654** (1999) 235c.
- [18] R. Kalpakchieva, Yu.E. Penionzhkevich, and H.G. Bohlen, Phys. Part. Nucl. **30** (1999) 627.
- [19] E. Caurier et al., Phys. Rev. C **59** (1999) 2033.
- [20] D.J. Dean et al., Phys. Rev. C **59** (1999) 2474.
- [21] T. Otsuka, T. Mizusaki, and M. Honma, J. Phys. G **25** (1999) 699.
- [22] E. Caurier et al., Phys. Rev. C **58** (1998) 2033.
- [23] A. Navin et al., Phys. Rev. Lett. **85** (2000) 266.
- [24] E.K. Warburton and B.A. Brown, Phys. Rev. C **46** (1992) 923.
- [25] J.M. Bang et al., Phys. Rep. **125** (1985) 253.
- [26] Y. Ogawa et al., Nucl. Phys. **A673** (2000) 122.
- [27] Y. Kanada-En'yo, H. Horiuchi, and A. Doté, Phys. Rev. C **60** (1999) 064304.
- [28] N. Itagaki and S. Okabe, Phys. Rev. C **61** (2000) 044306.
- [29] D. Baye, P. Descouvemont, and M. Hesse, Phys. Rev. C **58** (1998) 545.
- [30] J. Carlson and R. Schiavilla, Rev. Mod. Phys. **70** (1998) 743.
- [31] R.B. Wiringa, S.C. Pieper, J. Carlson, and V.R. Pandharipande, Phys. Rev. C **62** (2000) 014001.
- [32] R.B. Wiringa and R. Schiavilla, Phys. Rev. Lett. **81** (1998) 4317.
- [33] L. Lapikás, J. Wesseling, and R.B. Wiringa Phys. Rev. Lett. **82** (1999) 4404.
- [34] V.R. Pandharipande, I. Sick, and P.K.A. deWitt Huberts, Rev. Mod. Phys. **69** (1997) 981.
- [35] G.J. Kramer, H.P. Blok, and L. Lapikás, Nucl. Phys. **A679** (2001) 267.
- [36] P. Navrátil, and B.R. Barrett, Phys. Rev. C **57** (1998) 3119; P. Navrátil, J.P. Vary, and B.R. Barrett, Phys. Rev. Lett. **84** (2000) 5728.
- [37] F.C. Barker, Nucl. Phys. **83** (1966) 418.
- [38] S. Cohen and D. Kurath, Nucl. Phys. **73** (1965) 1.

- [39] J.B. French, E.C. Halbert, J.B. McGrory, and S.S.M. Wong, *Advances in Nuclear Physics* Vol. 3, Eds. M. Baranger and E.W. Vogt (Plenum Press, 1969), p. 193.
- [40] D.J. Millener in: *Group Theory and Special Symmetries in Nuclear Physics*, ed. J.P. Draayer, J. Jänecke (World Scientific, 1992), p. 276.
- [41] K. T. Hecht, *Annu. Rev. Nucl. Part. Sci.* **23** (1973) 123.
- [42] M.J.G. Borge et al., *Nucl. Phys.* **A460** (1986) 373.
- [43] M. Langevin et al., *Nucl. Phys.* **A366** (1981) 449.
- [44] D.J. Morrissey et al., *Nucl. Phys.* **A627** (1997) 222.
- [45] F.C. Barker and G.T. Hickey, *J. Phys. G* **3** (1977) L23.
- [46] T. Suzuki and T. Otsuka, *Phys. Rev. C* **56** (1997) 847.
- [47] T. Vertse, K. F. Pal and Z. Balogh, *Comp. Phys. Comm.* **27** (1982) 309.
- [48] H.A. Jahn and H. van Wieringen, *Proc. Roy. Soc.* **A209** (1951) 502.
- [49] S. Cohen and D. Kurath, *Nucl. Phys.* **A101** (1967) 1; *ibid.* **A141** (1970) 145; D. Kurath and D.J. Millener, *Nucl. Phys.* **A238** (1975) 269; D. Kurath, *Phys. Rev. C* **7** (1973) 1390.
- [50] J. Stevenson et al., *Phys. Rev. C* **37** (1988) 2220.
- [51] L. Chen et al., MSU preprint.
- [52] N.A.F.M. Popellier, A.A. Wolters, and P.W.M. Glaudemans, *Z. Phys. A* **346** 11; N.A.F.M. Popellier, Thesis, University of Utrecht, 1989.
- [53] A. Korsennikov et al., *Phys. Rev. Lett.* **82** (1999) 3581.
- [54] H.G. Bohlen et al., *Nuovo Cim.* **111 A** (1998) 841.
- [55] M. Thoennessen et al., *Phys. Rev. C* **59** (1999) 111.
- [56] J.A. Caggiano et al., *Phys. Rev. C* **60** (2000) 064322.
- [57] H. Simon et al., *Phys. Rev. Lett.* **83** (1999) 496.
- [58] D. Kurath and L. Pičman, *Nucl. Phys.* **10** (1959) 313.
- [59] J.P. Elliott and C.E. Wilsdon, *Proc. Roy. Soc. A* **302** (1958) 509.
- [60] I. Daito et al., *Phys. Lett. B* **418** (1998) 27.
- [61] F. Ajzenberg-Selove, *Nucl. Phys.* **A506** (1990) 1.
- [62] G.-B. Liu and H.T. Fortune, *Phys. Rev. C* **42** (1990) 167.
- [63] R.B. Weisenmiller et al., *Phys. Rev. C* **13** (1976) 1330.
- [64] R. Aryaeinejad et al., *Nucl. Phys.* **A436** (1985) 1.

- [65] A. Azhari et al., Phys. Rev. C **57** (1998) 628.
- [66] H.T. Fortune, G.-B. Liu, and D.E. Alburger, Phys. Rev. C **50** (1994) 1355.
- [67] D.J. Millener and D. Kurath, Nucl. Phys. **A255** (1975) 315.
- [68] W.D. Teeters and D. Kurath, Nucl. Phys. **A275** (1975) 61; *ibid.* **A283** (1977) 1.
- [69] D.J. Millener, D.E. Alburger, E.K. Warburton, and D.H. Wilkinson, Phys. Rev. C **26** (1982) 1167.
- [70] D.J. Millener, J.W. Olness, E.K. Warburton, and S.S. Hanna, Phys. Rev. C **28** (1983) 497.
- [71] D.H. Davis, Contemp. Phys. **27** (1986) 91; D.J. Millener, C.B. Dover, and A. Gal, Phys. Rev. C **38** (1988) 2700.
- [72] K. Markenroth et al., Phys. Rev. C **62** (2000) 034308.
- [73] J.M. Oliviera et al., Phys. Rev. Lett. **84** (2000) 4056.
- [74] B.A. Brown, W.A. Richter, and R. Lindsay, Phys. Lett. B **483** (2000) 49.
- [75] W. Geithner et al., Phys. Rev. Lett. **83** (1999) 3792.
- [76] T. Suzuki, T. Otsuka, and A. Muta, Phys. Lett. B **364** (1995) 69.
- [77] T. Aumann et al., Phys. Rev. Lett. **84** (2000) 35.
- [78] J.S. Winfield et al., Nucl. Phys. A **683** (2001) 48.
- [79] H. Iwasaki et al., Phys. Lett. B **491** (2000) 8.
- [80] A.N. Ostrowski et al., Z. Phys. A **343** (1992) 489.
- [81] A.V. Belozyorov et al., Nucl. Phys. **A636** (1998) 419.
- [82] G. Neyens et al., Phys. Rev. Lett. **82** (1999) 497; H. Ogawa et al., Phys. Lett. B **451** (1999) 11.
- [83] E. Sauvan et al., Phys. Lett. B **491** (2000) 1.
- [84] V. Maddalena et al., Phys. Rev. C **63** (2001) 024613.
- [85] D. Guimaraes et al., Phys. Rev. C **61** (2000) 064609.
- [86] R. Kalpakchieva et al., Eur. Phys. J. A **7** (2000) 451.
- [87] H. Okuno et al., Phys. Lett. B **354** (1995) 41; H. Izumi et al., Phys. Lett. B **366** (1996) 51; H. Ueno et al., Phys. Rev. C **53** (1996) 2142.
- [88] D.J. Millener, A.C. Hayes, and D. Strottman, Phys. Rev. C **45** (1992) 473.
- [89] E.K. Warburton, B.A. Brown, and D.J. Millener, Phys. Lett. B **293** (1992) 7.